

Influence of the angle between the wind and the isothermal surfaces on the boundary layer structures in turbulent thermal convection

Shishkina, O., Wagner, S. & Horn, S.

Published PDF deposited in Coventry University's Repository

Original citation:

Shishkina, O, Wagner, S & Horn, S 2014, 'Influence of the angle between the wind and the isothermal surfaces on the boundary layer structures in turbulent thermal convection' *Physical Review E*, vol. 89, 033014.

<https://dx.doi.org/10.1103/PhysRevE.89.033014>

DOI 10.1103/PhysRevE.89.033014

ISSN 1539-3755

ESSN 1550-2376

Publisher: American Physical Society

©2014 American Physical Society

Copyright © and Moral Rights are retained by the author(s) and/ or other copyright owners. A copy can be downloaded for personal non-commercial research or study, without prior permission or charge. This item cannot be reproduced or quoted extensively from without first obtaining permission in writing from the copyright holder(s). The content must not be changed in any way or sold commercially in any format or medium without the formal permission of the copyright holders.

Influence of the angle between the wind and the isothermal surfaces on the boundary layer structures in turbulent thermal convection

Olga Shishkina,^{*} Sebastian Wagner, and Susanne Horn

Institute of Aerodynamics and Flow Technology, German Aerospace Center (DLR), Bunsenstr a e 10, 37073 G ttingen, Germany

(Received 25 September 2013; published 21 March 2014)

We derive the asymptotes for the ratio of the thermal to viscous boundary layer thicknesses for infinite and infinitesimal Prandtl numbers Pr as functions of the angle β between the large-scale circulation and an isothermal heated or cooled surface for the case of turbulent thermal convection with laminar-like boundary layers. For this purpose, we apply the Falkner-Skan ansatz, which is a generalization of the Prandtl-Blasius one to a nonhorizontal free-stream flow above the viscous boundary layer. Based on our direct numerical simulations (DNS) of turbulent Rayleigh-B enard convection for $Pr = 0.1, 1, \text{ and } 10$ and moderate Rayleigh numbers up to 10^8 we evaluate the value of β that is found to be around 0.7π for all investigated cases. Our theoretical predictions for the boundary layer thicknesses for this β and the considered Pr are in good agreement with the DNS results.

DOI: [10.1103/PhysRevE.89.033014](https://doi.org/10.1103/PhysRevE.89.033014)

PACS number(s): 44.20.+b, 44.25.+f, 47.15.Cb, 47.27.te

I. INTRODUCTION

In turbulent thermal convection of fluids confined between a heated lower and a cooled upper horizontal plate, i.e., in Rayleigh-B enard convection (RBC), thermal boundary layers (BLs) occur at the plates and viscous BLs at all rigid walls. For moderate Rayleigh numbers $Ra = \tilde{\alpha}\tilde{g}\tilde{\Delta}\tilde{H}^3/(\tilde{\kappa}\tilde{\nu})$ ($\tilde{\alpha}$ denotes the isobaric thermal expansion coefficient, \tilde{g} the acceleration due to gravity, $\tilde{\Delta}$ the temperature difference between the plates, \tilde{H} their vertical distance, $\tilde{\nu}$ the kinematic viscosity, and $\tilde{\kappa}$ the thermal diffusivity), these BLs can be transitional or even laminar [1–5].

To approximate mean flow characteristics within the top and bottom BLs in this case, it is usually assumed that the wind of turbulence, or the so-called large-scale circulation (LSC), above the viscous BL is horizontal and constant, which corresponds to a zero pressure gradient. In contrast to this, recent direct numerical simulations (DNS) of turbulent RBC in different fluids showed that the wind is nonconstant along its path [6–8] and the time-averaged pressure gradient does not vanish [9].

In Shishkina *et al.* [10] we have shown that the Prandtl and Pohlhausen BL equations admit similarity solutions if the wind above the viscous BL follows either an exponential behavior or a power function. In the case of an exponential wind, the BL thickness decreases with the wind magnitude, whereas in the case of a power-function wind, the BL thickness increases with it. Based on our DNS of RBC in air and water, with Prandtl numbers $Pr = \tilde{\nu}/\tilde{\kappa} = 0.786$ and 4.38 , respectively, revealing that after the stagnation point the BL thickness grows with the wind magnitude, we concluded that in RBC only the wind obeying a power-law is relevant. This leads to the Falkner-Skan (FS) [11] momentum and Pohlhausen energy equations.

These equations account for a nonparallel wind or, in other words, for an angle β , $\beta < \pi$, between the LSC and the heated and cooled plate, and can be interpreted as an extension of the Prandtl-Blasius (PB) ansatz [12] to the case of a nonzero pressure gradient along the wind. In Shishkina *et al.* [10] we have evaluated the FS equations and the viscous BL thickness

for four particular values of β : π , $3\pi/4$, $2\pi/3$, and $\pi/2$. A comparison of the numerical solutions of the FS BL equations with our DNS data of water and air has shown that the FS approach leads to more accurate predictions of the BL thicknesses than the PB ansatz.

Here we give this idea more precision and derive several theoretical estimates. In Sec. II we present the numerical solution for the whole spectra of angles β . We now provide exact relations for the ratio of the thermal to viscous BL thicknesses in the limiting cases of $Pr \ll 1$ and $Pr \gg 1$ and also obtain the critical Prandtl number Pr^* for which the transition between these two regimes occurs.

Furthermore, we verify the FS approximation against DNS data for the generic Prandtl numbers $0.1, 1.0, \text{ and } 10.0$ (see Fig. 1), thus spanning three orders of magnitude in Pr . The BL properties for those Prandtl numbers are analyzed in Sec. III in a more sophisticated way, however, than in Ref. [10]. Instead of considering stationary LSC planes, we extract instantaneous LSC planes, hence, the potential movement of the direction of the LSC is taken into account as well.

Finally, in Sec. IV the mesh resolution requirements for the BLs in DNS are discussed. By employing the FS approximation instead of the PB one, the earlier estimates given in Shishkina *et al.* [13] are updated and improved.

II. FALKNER-SKAN-POHLHAUSEN BOUNDARY LAYERS

Following Prandtl [12] and Pohlhausen [14] and assuming that the wind and the free-fall velocity magnitudes are similar, from the full system of the 3D governing equations for RBC in Boussinesq approximation,

$$\tilde{\mathbf{u}}_t + \tilde{\mathbf{u}} \cdot \nabla \tilde{\mathbf{u}} + \tilde{\rho}^{-1} \nabla \tilde{p} = \tilde{\nu} \nabla^2 \tilde{\mathbf{u}} + \tilde{\alpha} \tilde{g} (\tilde{T} - \tilde{T}_{\text{mid}}) \hat{\mathbf{y}}, \quad (1)$$

$$\tilde{T}_t + \tilde{\mathbf{u}} \cdot \nabla \tilde{T} = \tilde{\kappa} \nabla^2 \tilde{T}, \quad \nabla \cdot \tilde{\mathbf{u}} = 0, \quad (2)$$

one obtains the following Prandtl (3) and Pohlhausen (4) equations [15] for laminar BLs:

$$\tilde{u}\tilde{u}_x + \tilde{v}\tilde{u}_y = \tilde{\nu}\tilde{u}_{yy} - \tilde{p}_x/\tilde{\rho}, \quad 0 = -\tilde{p}_y/\tilde{\rho}, \quad (3)$$

$$\tilde{u}\tilde{T}_x + \tilde{v}\tilde{T}_y = \tilde{\kappa}\tilde{T}_{yy}. \quad (4)$$

^{*}Olga.Shishkina@dlr.de

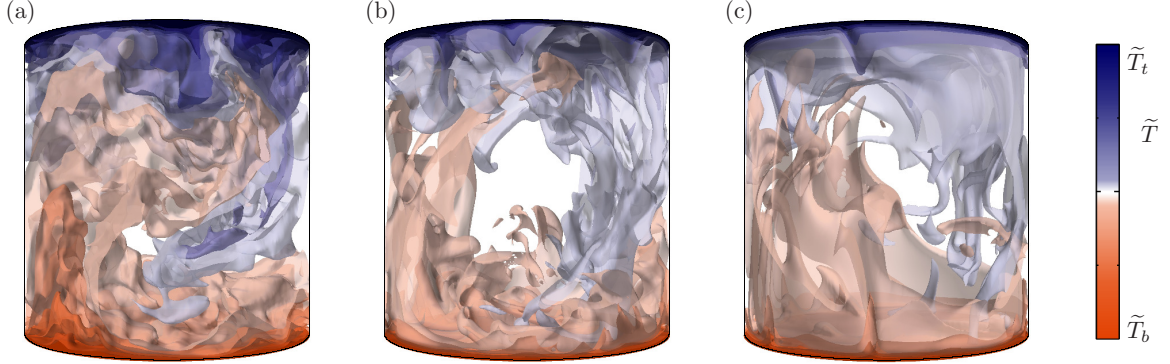


FIG. 1. (Color online) Instantaneous temperature fields obtained by DNS for $Ra = 10^8$ and (a) $Pr = 0.1$, (b) $Pr = 1$, and (c) $Pr = 10$ and presented with 10 isosurfaces for $\tilde{T} \in [\tilde{T}_t, \tilde{T}_b]$.

Here $\tilde{\mathbf{u}} \equiv (\tilde{u}, \tilde{v}, \tilde{w})^T$ is the velocity vector-function in the coordinate system $\tilde{\mathbf{x}} = (\tilde{x}, \tilde{y}, \tilde{z})$, \tilde{y} is the vertical direction, \tilde{x} and \tilde{z} are horizontal directions and \tilde{x} is along the wind, $\tilde{\mathbf{y}} \equiv (0, 1, 0)^T$, and \tilde{T} denotes the temperature, \tilde{p} the pressure, \tilde{T}_{mid} the arithmetic mean of the top (\tilde{T}_t) and bottom (\tilde{T}_b) temperatures, $\tilde{T}_t < \tilde{T}_b$, $\tilde{\rho}$ the density, and any variable marked as a subindex denotes the partial derivative with respect to this variable, e.g., $\tilde{u}_{\tilde{t}} \equiv \partial \tilde{u} / \partial \tilde{t}$, $\tilde{u}_{\tilde{x}} \equiv \partial \tilde{u} / \partial \tilde{x}$, $\tilde{u}_{\tilde{x}\tilde{x}} \equiv \partial^2 \tilde{u} / \partial \tilde{x}^2$. The vertical and horizontal walls of the container are assumed to be, respectively, adiabatic or isothermal and all of them are impermeable (no-slip boundary conditions). Note, that the Prandtl-Pohlhausen BL model [Eqs. (3), (4)] differs from that by Stewartson [16] for a very slow wind \tilde{U} above the viscous BL, $\tilde{U}^2 \ll \alpha \tilde{g} \tilde{\Delta} \tilde{L}$, with \tilde{L} being a representative length along the wind, where the buoyancy cannot be neglected. Since the considered BL flow is 2D and incompressible, Eqs. (3), (4) can be rewritten in terms of the streamfunction $\tilde{\Psi}$, which satisfies $\tilde{u} = \tilde{\Psi}_{\tilde{y}}$ and $\tilde{v} = -\tilde{\Psi}_{\tilde{x}}$. If a similarity solution is sought under the assumption that $\tilde{\Psi}$ and the similarity variable ξ are representable in the forms

$$\tilde{\Psi} = \tilde{v} \Psi(\xi) g(x), \quad \xi = y f(x), \quad (5)$$

and for the wind at the edge of the viscous BL holds $\tilde{U} = \tilde{U}(\tilde{x})$, then the similarity solution exists only if g_x/f is constant and g is either exponential or a power function of x [10]. Here $x \equiv \tilde{x}/\tilde{L}$ and $y \equiv \tilde{y}/\tilde{L}$ are the dimensionless spatial coordinates and the functions g and f depend on x alone. The case in which g is exponential describes a decreasing BL thickness along the wind, while if g is a power function, the BL thickness increases. The latter case is in good agreement with DNS results of turbulent RBC [8], which showed that near the horizontal plate, after the stagnation point, the BL thickness grows together with the wind magnitude. Thus, we consider only this case in the following. It leads to a BL of FS type [11], which develops for a corner flow with angle β along the corners' sides [cf. Fig. 4(a)]. In this case the core flow (or wind) above the BL and the pressure term within the BL equal, respectively,

$$\tilde{U} = \tilde{U}_0 x^{-1+\pi/\beta}, \quad (6)$$

$$-\tilde{p}_{\tilde{x}}/\tilde{\rho} = (\pi/\beta - 1) x^{-3+2\pi/\beta} \tilde{U}_0^2/\tilde{L}, \quad (7)$$

where \tilde{U}_0 is a constant velocity magnitude. If the wind is parallel to the horizontal plate, i.e., $\beta = \pi$, the FS BL is reduced to the PB one.

Thus, one obtains the following system of the dimensionless BL equations for the momentum (FS)

$$\Psi_{\xi\xi\xi} + \Psi \Psi_{\xi\xi} + (2 - \gamma)[1 - (\Psi_{\xi})^2] = 0, \quad (8)$$

$$\Psi(0) = 0, \quad \Psi_{\xi}(0) = 0, \quad \Psi_{\xi}(\infty) = 1, \quad (9)$$

and the energy

$$\Theta_{\xi\xi\xi} + Pr \Psi \Theta_{\xi} = 0, \quad (10)$$

$$\Theta(0) = 0, \quad \Theta(\infty) = 1. \quad (11)$$

For the similarity variable ξ , the stream function Ψ , and the dimensionless temperature Θ , the following expressions hold:

$$\xi \equiv \gamma^{-1/2} \text{Re}_0^{1/2} y x^{-1+1/\gamma}, \quad (12)$$

$$\Psi \equiv \gamma^{-1/2} \text{Re}_0^{-1/2} x^{-1/\gamma} \tilde{v}^{-1} \tilde{\Psi}, \quad (13)$$

$$\Theta \equiv 2(\tilde{T}_b - \tilde{T})/\tilde{\Delta}. \quad (14)$$

Here, $\text{Re}_0 \equiv \tilde{L}\tilde{U}_0/\tilde{v}$ is the Reynolds number based on the wind magnitude and

$$\gamma \equiv 2\beta/\pi. \quad (15)$$

With respect to the similarity variable ξ , the thickness of the viscous BL equals

$$\delta = (\Psi_{\xi}|_{\xi=0})^{-1} \quad (16)$$

and can be determined by solutions of the system of Eqs. (8) and (9). δ depends on γ and, hence, on the angle β . Taking $\xi = \delta$, $y = \tilde{\delta}_u/\tilde{L}$, where $\tilde{\delta}_u$ is the thickness of the viscous BL in physical space, from Eq. (12) one obtains

$$\tilde{\delta}_u/\tilde{L} = \delta \gamma^{1/2} \text{Re}_0^{-1/2} x^{1-1/\gamma}. \quad (17)$$

From Eqs. (6), (15), and (16) it follows that

$$\tilde{\delta}_u/\tilde{L} \sim \sqrt{x/\text{Re}}, \quad (18)$$

where the Reynolds number Re is based on the wind \tilde{U} [Eq. (6)]. Relation (18) holds for general Falkner-Skan BLs and thus also for the special case of Prandtl-Blasius BLs; i.e., $\gamma = 2$. The proportionality of the relative thickness of the boundary layer and the inverse square-root of the Reynolds number, commonly known as Prandtl formula, is one of the basic assumptions in the Grossmann-Lohse (GL) theory [1, 17, 18],

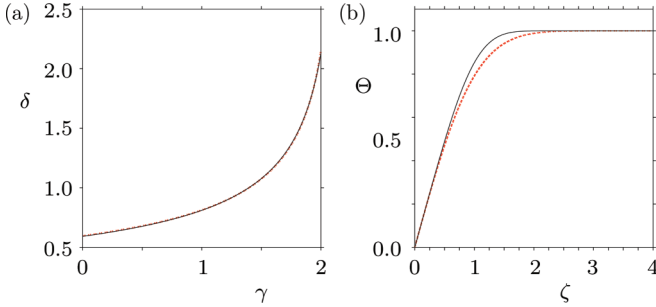


FIG. 2. (Color online) (a) Dependence on γ [Eq. (15)] of the viscous BL thickness δ with respect to the similarity variable ξ [Eq. (12)], as obtained from the numerical solutions of Eqs. (8) and (9) (—), and its approximation δ_{appr} (19) (---). (b) Limiting cases $\text{Pr} \ll 1$ (---) and $\text{Pr} \gg 1$ (—) of the rescaled temperature profile [Eqs. (23) and (24)] in the FS ansatz, for any angle β .

for the case of nonturbulent BLs. The latter theory estimates the dependence of the mean heat flux, expressed by the Nusselt number, on Ra and Pr . Since the more general case of the Prandtl formula (18) still holds for arbitrary γ , the scaling exponents in the theoretical estimates should remain unchanged, while considering Falkner-Skan BLs instead of Prandtl-Blasius BLs. Nevertheless, further estimates, which are based on the balance between the thermal and viscous BLs, may change when applying Falkner-Skan BLs, as we will elaborate below.

The dependence of the viscous BL δ on γ is obtained by solving numerically the system of FS Eqs. (8) and (9) for $0 \leq \gamma \leq 2$; i.e., for all angles $0 \leq \beta \leq \pi$ (see, e.g., Ref. [19], section 14.2). The result is presented in Fig. 2. It can be well approximated by

$$\delta \approx \delta_{\text{appr}} \equiv C_1(C_2 - \gamma)^{-1/2} \quad (19)$$

with $C_1 \approx 0.88$, $C_2 \approx 2.17$.

The temperature distributions within the BLs, i.e., the solution of the energy Eqs. (10) and (11) does not only depend on γ , but also on Pr . Using special similarity variables ζ as in Ref. [10], one obtains the temperature profiles for the limiting cases $\text{Pr} \ll 1$ and $\text{Pr} \gg 1$, which satisfy the boundary conditions

$$\Theta|_{\zeta=0} = 0, \quad \Theta_{\zeta}|_{\zeta=0} = 1, \quad \Theta|_{\zeta=\infty} = 1. \quad (20)$$

Thus, for the similarity variable

$$\zeta = C_3(\text{Pr})\gamma^{-1/2}\text{Re}_0^{1/2}yx^{-1+1/\gamma}, \quad (21)$$

with

$$C_3(\text{Pr}) = \begin{cases} 2^{1/2} \pi^{-1/2} \text{Pr}^{1/2}, & \text{Pr} \ll 1, \\ 6^{1/3} [\Gamma(4/3)]^{-1} \delta^{-1/3} \text{Pr}^{1/3}, & \text{Pr} \gg 1, \end{cases}$$

the limiting energy BL equations

$$\Theta_{\zeta\zeta} + (\pi/2)\zeta\Theta_{\zeta} = 0, \quad \text{Pr} \ll 1, \quad (22)$$

$$\Theta_{\zeta\zeta} + 3\Gamma^3(4/3)\zeta^2\Theta_{\zeta} = 0, \quad \text{Pr} \gg 1,$$

have the following solution,

$$\Theta(\zeta) = \int_0^{\zeta} \exp(-B\chi^{\omega}) d\chi, \quad (23)$$

with B and ω being constants defined as follows:

$$\begin{aligned} \omega = 2, \quad B = \pi/4, \quad \text{Pr} \ll 1, \\ \omega = 3, \quad B = \Gamma^3(4/3) \approx 0.71, \quad \text{Pr} \gg 1, \end{aligned} \quad (24)$$

and Γ being the gamma function. The limiting profiles (23) and (24) are independent of the angle β ; i.e., they are the same as in the PB case for all β [see Fig. 2(b)]. Further, for the thermal BL thickness $\tilde{\delta}_{\theta}$ in physical space, from Eqs. (20) and (21) one obtains

$$\tilde{\delta}_{\theta}/\tilde{L} = C_3^{-1} \gamma^{1/2} \text{Re}_0^{-1/2} x^{1-1/\gamma}. \quad (25)$$

The relations (17) and (25) give the ratio of the thermal to viscous BLs in the limiting cases $\text{Pr} \ll 1$ and $\text{Pr} \gg 1$, which depends only on the angle β and Prandtl number as

$$\begin{aligned} \tilde{\delta}_{\theta}/\tilde{\delta}_u &= [C_3(\text{Pr})\delta]^{-1} \\ &= \begin{cases} 2^{-1/2} \pi^{1/2} \text{Pr}^{-1/2} \delta^{-1}, & \text{Pr} \ll 1, \\ 6^{1/3} \Gamma(4/3) \text{Pr}^{-1/3} \delta^{-2/3}, & \text{Pr} \gg 1. \end{cases} \end{aligned} \quad (26)$$

Inserting the approximation (19), δ_{appr} , into the ratio (26), yields

$$\tilde{\delta}_{\theta}/\tilde{\delta}_u \approx C_4(\text{Pr})(C_2 - \gamma)^{1/\omega} \text{Pr}^{-1/\omega}, \quad (27)$$

with

$$\begin{aligned} \omega = 2, \quad C_4 \approx 1.43, \quad \text{Pr} \ll 1, \\ \omega = 3, \quad C_4 \approx 1.77, \quad \text{Pr} \gg 1. \end{aligned} \quad (28)$$

The derived asymptotes (27) and (28) are in excellent agreement with numerical results for some particular values of β , as reported in Ref. [10].

The change of the regime from $\text{Pr}^{-1/2}$ ($\text{Pr} \ll 1$) to $\text{Pr}^{-1/3}$ ($\text{Pr} \gg 1$) in Eq. (26) corresponds to the critical Prandtl number Pr^* , where the two asymptotes intersect. From Eqs. (26)–(28) we obtain that Pr^* can be approximated as follows:

$$\text{Pr}^* \approx 0.596 - 0.275\gamma, \quad (29)$$

which leads to $\text{Pr}^* \approx 0.046$ for the PB flow [13] and $\text{Pr}^* \approx 0.321$ for the stagnation-point flow.

For any particular γ and not extremely small or large Pr an approximation of $\tilde{\delta}_{\theta}/\tilde{\delta}_u$ can be obtained by applying a least square fit to the numerical solutions of the Eqs. (8)–(11) for the chosen γ and all possible Pr .

III. WIND IN TURBULENT RAYLEIGH-BÉNARD CONVECTION

In the following, the results of the previous section are verified against DNS of turbulent RBC in a cylindrical domain with a diameter-to-height aspect ratio of 1 for the Prandtl numbers $\text{Pr} = 0.1, 1$, and 10 and Ra up to 10^8 . The DNS were conducted using the same finite-volume code as in Ref. [20,21]. The DNS details can be found in Table I.

In the case of turbulent RBC for large enough Ra an LSC of fluid develops (see Fig. 3). Within the vertical LSC plane one obtains a large roll (LSC, wind) and two secondary rolls in the corners [Fig. 3(a)], while in the vertical LSC_{\perp} plane, which is orthogonal to the LSC plane, a four-roll structure develops [Fig. 3(b)]. From a large amount of instantaneous flow fields obtained in our DNS and sampled with a frequency of three

TABLE I. DNS parameters for different Pr and Ra: the number of mesh nodes in N_i direction ($i = r, \phi, z$) and in the thermal and viscous BLs as used in the DNS (n_T and n_u) and as estimated in Ref. [13] (\check{n}_T and \check{n}_u); Nusselt number Nu with its maximal deviation and the number of dimensionless time units τ used for the statistical averaging.

Pr	Ra	N_r	N_ϕ	N_z	n_T	\check{n}_T	n_u	\check{n}_u	Nu	τ
0.1	10^6	48	256	96	8	7	4	3	7.34 ± 0.10	295
	10^7	96	256	192	9	9	4	4	13.61 ± 0.08	506
	10^8	192	512	384	13	13	6	5	26.37 ± 0.64	68
1	10^6	48	256	96	7	2	7	2	8.60 ± 0.09	1231
	10^7	96	256	192	8	3	8	3	16.99 ± 0.16	1082
	10^8	192	512	384	11	4	11	4	32.60 ± 0.46	228
10	10^6	36	128	72	6	2	3	2	8.05 ± 0.03	3860
	10^7	64	512	128	5	3	4	3	16.43 ± 0.06	525
	10^8	192	512	384	9	4	11	4	32.50 ± 0.29	184

per time unit, we extract the wind direction. For this purpose we make use of the temperature distribution at the vertical wall at the height $\tilde{H}/2$ from the bottom [8,22]. Figure 4(b) sketches out the LSC and the secondary roll within the LSC plane near the bottom left corner of Fig. 3(a). There β can be understood as the angle between the wind and the heated bottom plate. The value of β is determined by the locations, where the wall shear stress at the vertical and horizontal walls at the sides of the corner is equal to zero (see Fig. 5). Our DNS of turbulent RBC for different Ra and Pr show that β varies around 0.7π ,

$$\beta = \begin{cases} 0.69\pi \pm 0.02\pi, & \text{Pr} = 0.1, \\ 0.71\pi \pm 0.02\pi, & \text{Pr} = 1, \\ 0.71\pi \pm 0.03\pi, & \text{Pr} = 10, \end{cases} \quad (30)$$

and is similar to the angles obtained earlier for Pr = 0.786 and 4.38 and Ra between 10^7 and 10^9 [10].

Thus, for $\gamma = 1.4$, which corresponds to $\beta = 0.7\pi$, we obtain

$$\frac{\tilde{\delta}_\theta}{\tilde{\delta}_u} \approx \begin{cases} 1.25\text{Pr}^{-1/2}, & \text{Pr} < 10^{-4}, \\ 1.75\text{Pr}^{-0.395+0.017 \log \text{Pr}}, & 10^{-4} \leq \text{Pr} \leq 10^3, \\ 1.62\text{Pr}^{-1/3}, & 10^3 < \text{Pr}, \end{cases} \quad (31)$$

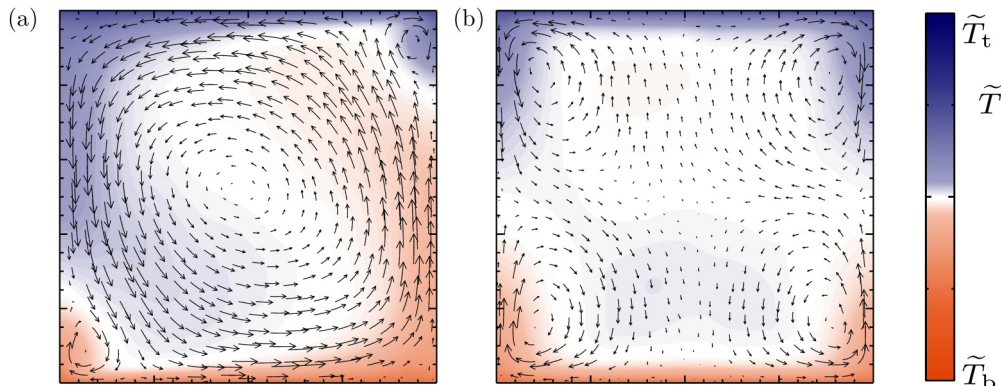


FIG. 3. (Color online) Time-averaged temperature field with superposed velocity vectors in the vertical (a) LSC-plane and (b) LSC $_{\perp}$ -plane, as obtained in DNS of turbulent RBC for Ra = 10^7 and Pr = 0.1 (see Table I for the DNS details).

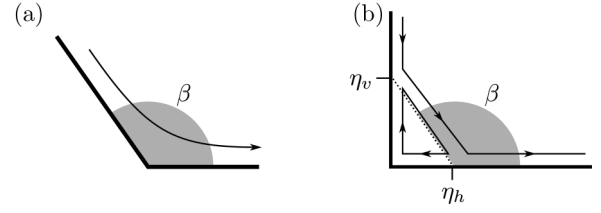


FIG. 4. (a) Sketch of the corner flow with opening angle β in the FS sense. (b) Sketch of the LSC and secondary roll within the LSC plane near the bottom left corner of Fig. 3(a). Here, η_v and η_h are the distances from the corner to the locations, where the wall shear stress equals zero, and β is the angle at which the LSC attacks the heated bottom plate.

where $\log \equiv \log_{10}$ is the logarithm to base ten. The estimate (31) gives $\tilde{\delta}_\theta/\tilde{\delta}_u \approx 4.52$ (Pr = 0.1), $\tilde{\delta}_\theta/\tilde{\delta}_u \approx 1.75$ (Pr = 1), and $\tilde{\delta}_\theta/\tilde{\delta}_u \approx 0.73$ (Pr = 10).

We compare these predictions with the ratios $\langle \tilde{\delta}_\theta/\tilde{\delta}_u \rangle_{\tilde{r}}$ along the wind near the bottom plate, obtained in our DNS. (Here $\langle \dots \rangle_{\tilde{r}}$ denotes the time averaging.) Similar to Shi *et al.* [9], we consider the instantaneous LSC plane and evaluate the viscous and thermal BL thicknesses by using the slope method [8]. The wind velocity is determined as the maximum of the radial velocity considered at heights smaller than $2\tilde{H}/\text{Nu}(\tilde{\delta}_\theta/\tilde{\delta}_u)^{-1}$, where $\tilde{\delta}_\theta/\tilde{\delta}_u$ is estimated within the PB ansatz (i.e., $\beta = \pi$).

Note that in Ref. [8] the maximum considered height for evaluating the wind magnitude was $2\tilde{H}/\text{Nu}$, since there Pr was close to one and, consequently, $\tilde{\delta}_\theta/\tilde{\delta}_u$ was approximately one as well.

The resulting ratios $\langle \tilde{\delta}_\theta/\tilde{\delta}_u \rangle_{\tilde{r}}$ are presented in Fig. 6 in dependence of the horizontal position x/H , for different Pr and Ra, together with the estimates (horizontal lines) for $\beta = \pi$ (Prandtl-Blasius flow), $\beta = \pi/2$ (stagnation-point flow) [10], and $\beta = 0.7\pi$ [Eq. (31)]. As one can see, the ratios remain almost constant along the path of the wind. The prediction for $\beta = 0.7\pi$ represents the DNS results generally better than the classical PB ansatz ($\beta = \pi$) [10].

However, one of the key assumptions of the developed approach is a strong enough wind, i.e., buoyancy can be neglected within the BLs cf. Ref. [10]. Hence, for small Prandtl numbers, the agreement with the theory is better for larger Rayleigh numbers, when the wind dominates over

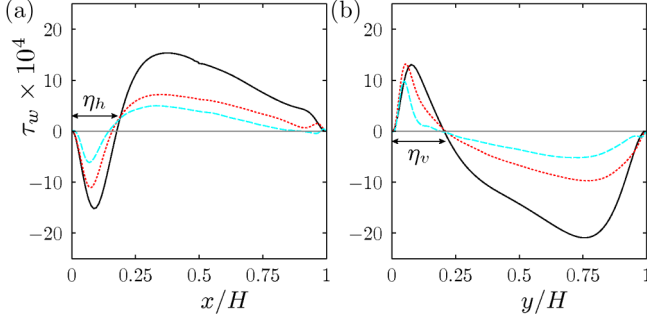


FIG. 5. (Color online) Dimensionless time-averaged wall shear stress (a) at the bottom, $\tau_w = \frac{\tilde{H}^2}{\text{Ra}\tilde{\kappa}} \langle \frac{\partial \tilde{v}}{\partial \tilde{x}} \rangle_{\tilde{t}}$, and (b) left vertical wall in the LSC plane, $\tau_w = \frac{\tilde{H}^2}{\text{Ra}\tilde{\kappa}} \langle \frac{\partial \tilde{u}}{\partial \tilde{y}} \rangle_{\tilde{t}}$, as obtained in the DNS for $\text{Pr} = 1$ and 10^6 (—), 10^7 (· ·), and 10^8 (- -) with η_v and η_h as in Fig. 4(b).

the small-scale fluctuations. This is evident from Fig. 6(a) for $\text{Pr} = 0.1$. For $\text{Ra} = 10^6$ and 10^7 the strong small-scale fluctuations lead to a small over-prediction of the ratio $\langle \tilde{\delta}_\theta / \tilde{\delta}_u \rangle_{\tilde{t}}$, whereas for $\text{Ra} = 10^8$ a fair agreement is found. For larger Prandtl numbers, as in the case of $\text{Pr} = 10$ displayed in Fig. 6(c), the wind itself is not strong enough, hence the ratio $\langle \tilde{\delta}_\theta / \tilde{\delta}_u \rangle_{\tilde{t}}$ is slightly under-predicted.

Nonetheless, the prediction given by Eq. (31) is always in a better agreement with the DNS data than the PB one.

IV. CONSEQUENCES FOR THE GRID RESOLUTION IN DNS

In this section we discuss shortly the influence of wind angle on the required grid resolution in DNS of turbulent thermal convection.

It is the well-established criterion [13] that in DNS the (local) mesh size \tilde{h} must not be larger than the (local)

Kolmogorov $\tilde{\eta}_K(\tilde{\mathbf{x}}, t)$ [23] and Batchelor $\tilde{\eta}_B$ [24] scales:

$$\tilde{\eta}_K(\tilde{\mathbf{x}}, \tilde{t}) = [\tilde{v}^3 / \tilde{\epsilon}_u(\tilde{\mathbf{x}}, \tilde{t})]^{1/4}, \quad (32)$$

$$\tilde{\eta}_B(\tilde{\mathbf{x}}, \tilde{t}) = [\tilde{v}\tilde{\kappa}^2 / \tilde{\epsilon}_u(\tilde{\mathbf{x}}, \tilde{t})]^{1/4} = \tilde{\eta}_K(\tilde{\mathbf{x}}, \tilde{t})\text{Pr}^{-1/2}, \quad (33)$$

which are defined with the kinetic energy dissipation rate

$$\tilde{\epsilon}_u(\tilde{\mathbf{x}}, \tilde{t}) \equiv \frac{\tilde{v}}{2} \sum_i \sum_j \left[\frac{\partial \tilde{u}_i(\tilde{\mathbf{x}}, \tilde{t})}{\partial \tilde{x}_j} + \frac{\partial \tilde{u}_j(\tilde{\mathbf{x}}, \tilde{t})}{\partial \tilde{x}_i} \right]^2, \quad (34)$$

where $(\tilde{x}_1, \tilde{x}_2, \tilde{x}_3) \equiv (\tilde{x}, \tilde{y}, \tilde{z})$. In a horizontal plane A within the viscous BL the energy dissipation rate $\tilde{\epsilon}_u|_{A \in BL}$ can be approximated as

$$\tilde{\epsilon}_u|_{A \in BL} \approx \tilde{v}(\tilde{U}/\tilde{\delta}_u)^2. \quad (35)$$

From this and Eqs. (17), (19), and (32) we obtain the following estimate for $\tilde{\eta}_K|_{A \in BL}$:

$$\frac{\tilde{\eta}_K|_{A \in BL}}{\tilde{L}} \approx \left(\frac{\gamma}{C_2 - \gamma} \frac{C_1^2 x}{\text{Re}^3} \right)^{1/4}, \quad (36)$$

where $\text{Re} \equiv \tilde{L}\tilde{U}/\tilde{v}$ is the Reynolds number based on the wind Eq. (6).

Therefore, for similar Reynolds numbers, near the isothermal plate, the required mesh size \tilde{h}_{sp} for the stagnation point flow ($\gamma = \gamma_{\text{sp}} \equiv 1$) is related to the mesh size \tilde{h}_{PB} for the PB flow ($\gamma = \gamma_{\text{PB}} \equiv 2$) by

$$\frac{\tilde{h}_{\text{PB}}}{\tilde{h}_{\text{sp}}} \approx \left(\frac{\gamma_{\text{PB}}}{C_2 - \gamma_{\text{PB}}} \frac{C_2 - \gamma_{\text{sp}}}{\gamma_{\text{sp}}} \right)^{1/4} \approx 1.93. \quad (37)$$

This means that in DNS of turbulent thermal convection, in which the wind is not everywhere parallel to the isothermal plate (like in RBC), an up to two times finer mesh resolution than in the case of PB BLs is required within the BLs.

V. CONCLUSIONS

To describe laminar boundary layers in thermal convection, we considered a generalization of the Prandtl-Blasius ansatz to the case of a nonhorizontal free-stream flow above the viscous boundary layer, i.e., the Falkner-Skan ansatz [10].

The asymptotes for the ratio of the thermal to viscous boundary layer thicknesses for infinite and infinitesimal Prandtl numbers were derived as functions of the angle β between the wind and the isothermal horizontal plate.

DNS of turbulent RBC for $\text{Pr} = 0.1, 1, \text{ and } 10$ and Rayleigh numbers up to 10^8 showed that $\beta \approx 0.7\pi$ for all investigated cases. The predictions for the boundary layer thicknesses for this β and the considered Pr are found to be in better agreement with the DNS results than the Prandtl-Blasius ones.

Since the developed approach is based on the assumption of a relatively strong wind above the viscous boundary layer, which is compatible with the free-fall velocity, the agreement of the theoretical estimates and the DNS results is best for relatively large Rayleigh numbers, $\text{Ra} \gtrsim 10^8$, and small Prandtl numbers, $\text{Pr} \lesssim 1$. For smaller Ra and higher Pr there is an apparent deviation between theory and DNS, because this prerequisite is less valid. Nonetheless, even in those cases the theoretical predictions based on the Falkner-Skan

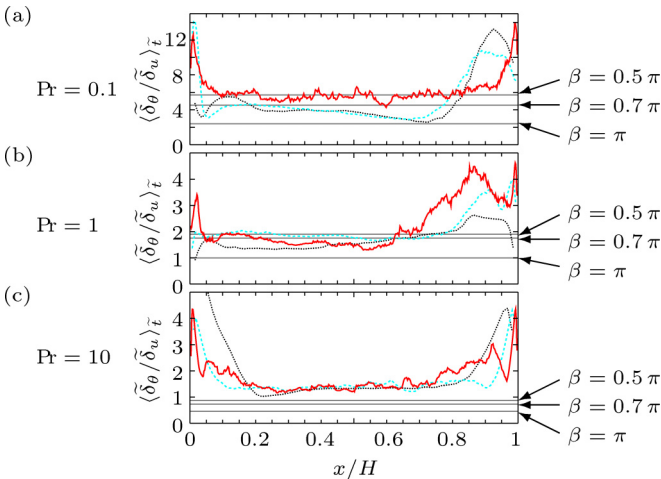


FIG. 6. (Color online) Ratio $\langle \tilde{\delta}_\theta / \tilde{\delta}_u \rangle_{\tilde{t}}$ of the thermal and viscous BL thicknesses for (a) $\text{Pr} = 0.1$, (b) $\text{Pr} = 1$, (c) $\text{Pr} = 10$, as obtained in the DNS for $\text{Ra} = 10^8$ (—), 10^7 (- -), and 10^6 (· ·) together with the predictions [10] (gray horizontal lines) for $\beta = \pi$ (Prandtl-Blasius flow), $\beta = \pi/2$ (stagnation-point flow), and estimate (31) for $\beta = 0.7\pi$.

ansatz result in a better agreement than those based on the Prandtl-Blasius ansatz.

It is also expected that in mixed convection with imposed free-stream flows, moderate Rayleigh numbers and Archimedes numbers about one, even better agreement of the theoretical predictions and DNS or experimental results can be obtained. This and measurements [25] of the BL thicknesses along the path of the large-scale circulation near

the isothermal surfaces might be the subject of forthcoming studies.

ACKNOWLEDGMENTS

The authors acknowledge financial support of the Deutsche Forschungsgemeinschaft (DFG) under Grants SH405/2, SH405/3, and SFB963/1, project A6.

-
- [1] S. Grossmann and D. Lohse, *J. Fluid Mech.* **407**, 27 (2000).
- [2] B. Eckhardt, S. Grossmann, and D. Lohse, in *Progress in Turbulence II*, Springer Proceedings in Physics, Vol. 109, edited by M. Oberlack, G. Khujudze, S. Günther, T. Weller, M. Frewer, J. Peinke, and S. Barth (Springer Verlag, Berlin, 2007), pp. 3–10.
- [3] G. Ahlers, S. Grossmann, and D. Lohse, *Rev. Mod. Phys.* **81**, 503 (2009).
- [4] D. Lohse and K.-Q. Xia, *Annu. Rev. Fluid Mech.* **42**, 335 (2010).
- [5] F. Chillà and J. Schumacher, *Eur. Phys. J. E* **35**, 58 (2012).
- [6] M. Kaczorowski, O. Shishkina, A. Shishkin, C. Wagner, and K.-Q. Xia, in *Direct and Large-Eddy Simulation VIII*, edited by H. Kuerten, B. Geurts, V. Armenio, and J. Fröhlich (Springer, Berlin, 2011), pp. 383–388.
- [7] O. Shishkina and C. Wagner, *J. Fluid Mech.* **686**, 568 (2011).
- [8] S. Wagner, O. Shishkina, and C. Wagner, *J. Fluid Mech.* **697**, 336 (2012).
- [9] N. Shi, M. S. Emran, and J. Schumacher, *J. Fluid Mech.* **706**, 5 (2012).
- [10] O. Shishkina, S. Horn, and S. Wagner, *J. Fluid Mech.* **730**, 442 (2013).
- [11] V. M. Falkner and S. W. Skan, *Phil. Mag.* **12**, 865 (1931).
- [12] L. Prandtl, in *Verhandlungen des III. Int. Math. Kongr., Heidelberg, 1904* (Teubner, Leipzig, 1905), pp. 484–491.
- [13] O. Shishkina, R. J. A. M. Stevens, S. Grossmann, and D. Lohse, *New J. Phys.* **12**, 075022 (2010).
- [14] K. Pohlhausen, *Z. Angew. Math. Mech.* **1**, 252 (1921).
- [15] H. Schlichting and K. Gersten, *Boundary-Layer Theory*, 8th ed. (Springer, Berlin, 2000).
- [16] K. Stewartson, *Z. angew. Math. Phys.* **16**, 276 (1958).
- [17] S. Grossmann and D. Lohse, *Phys. Rev. Lett.* **86**, 3316 (2001).
- [18] R. J. A. M. Stevens, E. P. van der Poel, S. Grossmann, and D. Lohse, *J. Fluid Mech.* **730**, 295 (2013).
- [19] D. C. Wilcox, *Basic Fluid Mechanics*, 4th ed. (DCW Industries, La Canada, CA, 2010).
- [20] O. Shishkina and C. Wagner, *C. R. Mecanique* **333**, 17 (2005).
- [21] S. Horn, O. Shishkina, and C. Wagner, *J. Fluid Mech.* **724**, 175 (2013).
- [22] E. Brown and G. Ahlers, *J. Fluid Mech.* **568**, 351 (2006).
- [23] A. N. Kolmogorov, *Dokl. Akad. Nauk. SSSR.* **30**, 299 (1941).
- [24] G. K. Batchelor, *J. Fluid Mech.* **5**, 113 (1959).
- [25] L. Li, N. Shi, R. du Puits, C. Resagk, J. Schumacher, and A. Thess, *Phys. Rev. E* **86**, 026315 (2012).